

GaAs-based air-slot photonic crystal nanocavity for optomechanical oscillators

Masahiro Nomura*

Institute of Industrial Science, The University of Tokyo, Tokyo 153-8505, Japan
Institute for Nano Quantum Information Electronics, The University of Tokyo, Tokyo 153-8505, Japan
nomura@iis.u-tokyo.ac.jp

Abstract: We theoretically investigate an optomechanical structure consisting of two parallel GaAs membranes with an air-slot type photonic crystal nanocavity. The optical cavity has a quality factor of 4.8×10^6 at $1.52 \mu\text{m}$ and an extremely small modal volume of 0.015 of a cubic wavelength for the fundamental mode in a vacuum. The localized electric field near the air/dielectric-object boundary provides a large optomechanical coupling factor of $\sim 990 \text{ GHz/nm}$. The fundamental mechanical mode resonance is 95 MHz and a quality factor is 83,800 at room temperature, nearly seven times higher than that for a similar Si-based structure. This high mechanical quality factor of a GaAs-based structure stems from low thermoelastic loss and leads to more effective optical control of nanomechanical oscillators.

© 2012 Optical Society of America

OCIS codes: (120.4880) Optomechanics; (050.5298) Photonic crystals; (140.3320) Laser cooling; (140.3945) Microcavities.

References and links

1. F. Diedrich, J. C. Bergquist, W. M. Itano, and D. J. Wineland, "Laser cooling to the zero-point energy of motion," *Phys. Rev. Lett.* **62**(4), 403–406 (1989).
2. C. N. Cohen-Tannoudji and W. D. Phillips, "New mechanisms for laser cooling," *Phys. Today* **43**(10), 33–40 (1990).
3. S. Chu, "Laser manipulation of atoms and particles," *Science* **253**(5022), 861–866 (1991).
4. V. Braginsky and A. Manukin, *Measurement of Weak Forces in Physics Experiments* (Univ. Chicago Press, 1977).
5. T. J. Kippenberg and K. J. Vahala, "Cavity optomechanics: back-action at the mesoscale," *Science* **321**(5893), 1172–1176 (2008).
6. D. Van Thourhout and J. Roels, "Optomechanical Device actuation through the optical gradient force," *Nat. Photonics* **4**(4), 211–217 (2010).
7. D. Kleckner and D. Bouwmeester, "Sub-kelvin optical cooling of a micromechanical resonator," *Nature* **444**(7115), 75–78 (2006).
8. C. H. Metzger and K. Karrai, "Cavity cooling of a microlever," *Nature* **432**(7020), 1002–1005 (2004).
9. J. D. Thompson, B. M. Zwickl, A. M. Jayich, F. Marquardt, S. M. Girvin, and J. G. E. Harris, "Strong dispersive coupling of a high-finesse cavity to a micromechanical membrane," *Nature* **452**(7183), 72–75 (2008).
10. O. Arcizet, P. F. Cohadon, T. Briant, M. Pinard, and A. Heidmann, "Radiation-pressure cooling and optomechanical instability of a micromirror," *Nature* **444**(7115), 71–74 (2006).
11. G. Anetsberger, O. Arcizet, Q. P. Unterreithmeier, R. Riviere, A. Schliesser, E. M. Weig, J. P. Kotthaus, and T. J. Kippenberg, "Near-field cavity optomechanics with nanomechanical oscillators," *Nat. Phys.* **5**(12), 909–914 (2009).
12. Y.-S. Park and H. Wang, "Resolved-sideband and cryogenic cooling of an optomechanical resonator," *Nat. Phys.* **5**(7), 489–493 (2009).
13. M. Eichenfield, R. Camacho, J. Chan, K. J. Vahala, and O. Painter, "A picogram- and nanometre-scale photonic-crystal optomechanical cavity," *Nature* **459**(7246), 550–555 (2009).
14. J. Chan, T. P. M. Alegre, A. H. Safavi-Naeini, J. T. Hill, A. Krause, S. Gröblacher, M. Aspelmeyer, and O. Painter, "Laser cooling of a nanomechanical oscillator into its quantum ground state," *Nature* **478**(7367), 89–92 (2011).
15. Y. Li, J. Zheng, J. Gao, J. Shu, M. S. Aras, and C. W. Wong, "Design of dispersive optomechanical coupling and cooling in ultrahigh- Q/V slot-type photonic crystal cavities," *Opt. Express* **18**(23), 23844–23856 (2010).

16. J. Gao, J. F. McMillan, M.-C. Wu, J. Zheng, S. Assefa, and C. W. Wong, "Demonstration of an air-slot modegap confined photonic crystal slab nanocavity with ultrasmall mode volumes," *Appl. Phys. Lett.* **96**(5), 051123 (2010).
17. A. H. Safavi-Naeini, T. P. M. Alegre, M. Winger, and O. Painer, "Optomechanics in an ultrahigh-Q two-dimensional photonic crystal cavity," *Appl. Phys. Lett.* **97**(18), 181106 (2010).
18. T. Yoshie, A. Scherer, J. Hendrickson, G. Khitrova, H. M. Gibbs, G. Rupper, C. Ell, O. B. Shchekin, and D. G. Deppe, "Vacuum Rabi splitting with a single quantum dot in a photonic crystal nanocavity," *Nature* **432**(7014), 200–203 (2004).
19. M. Nomura, N. Kumagai, S. Iwamoto, Y. Ota, and Y. Arakawa, "Laser oscillation in a strongly coupled single quantum dot-nanocavity system," *Nat. Phys.* **6**(4), 279–283 (2010).
20. L. Ding, C. Baker, P. Senellart, A. Lemaitre, S. Ducci, G. Leo, and I. Favero, "High frequency GaAs nano-optomechanical disk resonator," *Phys. Rev. Lett.* **105**(26), 263903 (2010).
21. H. Okamoto, D. Ito, K. Onomitsu, H. Sanada, H. Gotoh, T. Sogawa, and H. Yamaguchi, "Vibration amplification, damping, and self-oscillations in micromechanical resonators induced by optomechanical coupling through carrier excitation," *Phys. Rev. Lett.* **106**(3), 036801 (2011).
22. E. Kuramochi, M. Notomi, S. Mitsugi, A. Shinya, T. Tanabe, and T. Watanabe, "Ultra-high-Q photonic crystal nanocavities realized by the local width modulation of a line defect," *Appl. Phys. Lett.* **88**(4), 041112 (2006).
23. T. Yamamoto, M. Notomi, H. Taniyama, E. Kuramochi, Y. Yoshikawa, Y. Torii, and T. Kuga, "Design of a high-Q air-slot cavity based on a width-modulated line-defect in a photonic crystal slab," *Opt. Express* **16**(18), 13809–13817 (2008).
24. Z. Zhang and M. Qiu, "Small-volume waveguide-section high Q microcavities in 2D photonic crystal slabs," *Opt. Express* **12**(17), 3988–3995 (2004).
25. H. S. Ee, K. Y. Jeong, M. K. Seo, Y. H. Lee, and H. G. Park, "Ultrasmall square-lattice zero-cell photonic crystal laser," *Appl. Phys. Lett.* **93**(1), 011104 (2008).
26. M. Nomura, K. Tanabe, S. Iwamoto, and Y. Arakawa, "High- Q design of semiconductor-based ultrasmall photonic crystal nanocavity," *Opt. Express* **18**(8), 8144–8150 (2010).
27. C. Zener, "Internal Friction in Solids. I. Theory of Internal Friction in Reeds," *Phys. Rev.* **52**(3), 230–235 (1937).
28. T. H. Metcalf, B. B. Pate, D. M. Photiadis, and B. H. Houston, "Thermoelastic damping in micromechanical resonators," *Appl. Phys. Lett.* **95**(6), 061903 (2009).

1. Introduction

It has been known that atoms and ions can be mechanically manipulated by a nearly resonant laser beam [1–3] and even massive dielectric objects can be optically manipulated via the radiation-pressure and the optical gradient force [4]. Recently, the optical manipulation of micro and nanomechanical structures has been intensively investigated due to interests in both the fundamental physics and a variety of potential applications, including highly sensitive mass and weak force detections. In experimental investigations, cavity-assisted schemes are used to enhance the interaction between a mechanical oscillator and a resonant electric field. Optomechanical experiments using the radiation pressure [5] or the optical gradient force [6] have been performed using a microlever with a micromirror [7, 8], a thin membrane in or as an optical cavity [9, 10], a micro toroid [11], a microsphere [12], and a photonic crystal (PhC) [13, 14] structure. The optical gradient force, which is the basic operation principle of optical tweezers, can provide a much larger force per photon when strong field gradients are available. Therefore, the optical gradient force can be used for efficient manipulation of optomechanical systems. The origin of the optical gradient force can be understood interaction between the gradient field and an electric dipole in a structure induced by the gradient field.

There are several key issues for optomechanical systems using the cavity enhanced optical gradient force: optical quality factor (Q), modal volume (V), mechanical quality factor (Q_m), and optomechanical coupling strength. The damping of the optical and mechanical modes should be reduced and optomechanical coupling should be stronger to achieve efficient optomechanical systems. The electric field distribution of the optical mode is also an important issue. The electric field maximum and displacement field maximum should be located at the same position for more efficient optomechanical coupling. In addition, the electric field distribution should have large gradient near the air/dielectric-object boundary so that the electric field can affect the motion of the object. An air-slot semiconductor PhC nanocavity, which has a localized electric field around air/dielectric-object boundary, fulfills these essential prerequisites and therefore it is one of the good candidates for an

optomechanical system using a cavity enhanced scheme. Recently, high optomechanical performance of a Si-based structure with an air-slot PhC nanocavity has been theoretically predicted [15] and the experiments have been performed using Si [16, 17]. GaAs-based PhC nanocavities, on the other hand, have mostly been designed so that the cavity electric field maximum is located in the dielectric material to investigate light-matter interaction [18] or achieve laser oscillation with low dimensional quantum structures [19]. There are some reports on GaAs-based optomechanical resonators using a microdisk resonator [20] and a cantilever [21]. However, to the best of our knowledge, there is no report that investigates optomechanical properties of the air-slot type PhC nanocavity with GaAs material.

In this paper, we theoretically investigate optomechanical coupling between a pair of GaAs membranes with an air-slot mode-gap PhC nanocavity and the optical mode. Numerically estimated optical properties, mechanical properties, and optomechanical properties of a designed structure are shown. We analyzed the motion of the nanomechanical oscillator controlled by a slightly detuned single-frequency pump laser. Then, we show the advantage of a GaAs-based structure over a Si-based structure in mechanical property and the importance of the mechanical property in optomechanical control of damping and amplification of the mechanical oscillator.

2. Structure of nanomechanical oscillator

Figure 1 shows a schematic of the investigated nanostructure consisting of two parallel GaAs membrane separated by an air-slot with a width $s = 80$ nm, which is located at the center of a line defect (W1) of a triangular lattice of air-holes. The period of the lattice a and the radius of the air-hole r are 490 nm and 140 nm, respectively. The thickness, length and width of the membrane are 204 nm, $7.84 \mu\text{m}$ ($16a$), and $2.08 \mu\text{m}$ ($2.5\sqrt{3}a - s/2$). The nanomechanical structure possesses a mode-gap type photonic crystal (PhC) cavity with a high Q [22] to enhance the optomechanical coupling by a long cavity photon lifetime. The air-holes are slightly shifted outward as indicated in the inset by arrows in Fig. 1(a) to create a mode-gap PhC nanocavity. The amounts of shifts are 3δ , 2δ , and δ for the air-holes as respectively indicated by red, blue, and green arrows, where $\delta = 0.0095a$. This cavity design was proposed by Yamamoto *et al.* for the study of cavity quantum electrodynamics in free space with Si-based structures [23]. We note that air-slot type cavities are also useful for optomechanics, and actually, possibility of operation in a resolved-sideband limit is theoretically reported in [15]. In this structure, photons are localized at the air-semiconductor boundary. Therefore, the cavity field is sensitive to the motion of the semiconductor membranes, and the optomechanical coupling strength is expected to be very high.

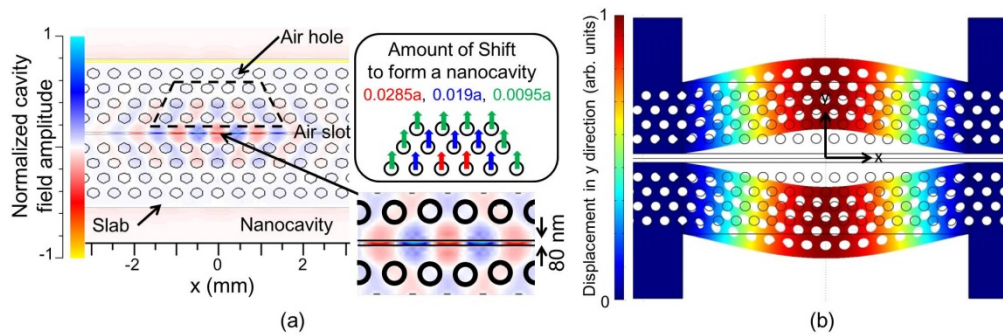


Fig. 1. (a) Computed cavity electric field distribution in the air-slot PhC nanocavity structure. The long-term ($Q = 4.8 \times 10^6$) and localized ($V = 0.015\lambda^3$) electric field confinement around the air/semiconductor boundary results in extremely strong optomechanical interaction. (b) Color plot of the absolute displacement in y direction for the investigated fundamental mechanical oscillation mode (95 MHz). This oscillation can be optically controlled by the cavity field in the PhC nanocavity.

3. Simulation results and discussions

In this section, we report optical properties of the air-slot mode-gap PhC nanocavity, mechanical properties of the doubly clamped GaAs membrane, and optomechanical coupling of the GaAs nanomechanical oscillator with the PhC nanocavity. The motion of the GaAs membrane is analyzed by the estimated parameters. Then, the performance as an optomechanical oscillator of a GaAs-based structure is compared with that of a similar Si-based structure.

3.1 Optical properties

Three-dimensional finite-difference time-domain method was performed to investigate optical properties of the designed air-slot mode-gap PhC cavity in a pair of GaAs membranes. Even symmetry conditions were set in x - y and x - z planes to select a preferred even mode for the electric field: the axes are defined in Fig. 1. The spatial distribution of the calculated electric field amplitude for the fundamental transverse mode, which is found at 1518 nm, is shown in Fig. 1(a). This cavity supports single mode within the wavelength range of the research interest due to its small cavity dimension. The optomechanical coupling of this mode and the in-plane fundamental mechanical mode, which will be shown in the next section, is studied in this paper. The air-slot plays an essential role for the localization of the electric field due to the conservation of the electric flux density in the normal direction of the air/semiconductor boundary. Therefore, the electric field is enhanced by a factor of the dielectric constant ϵ in the air-slot compared with the electric field in an adjacent semiconductor membrane, where $\epsilon = 11.42$ for the studied GaAs membrane at the cavity resonance. The lower right inset in Fig. 1 clearly shows that the electric field in the air-slot is much higher than that in the semiconductor membrane. The calculated value of the cavity Q is $\sim 4.8 \times 10^6$ and the modal volume of this mode V is $\sim 0.015\lambda^3$: λ is the wavelength of the cavity mode. The small V is smaller than that of PhC nanocavities without air-slots by more than one order of magnitude [24–26]. The high value of Q confines the electric fields for long time and enables efficient optomechanical coupling with low pumping power. The small V leads to high displacement sensitivity for the motion of the membrane in the in-plane direction. The coupling of photons from a control light source into this small cavity can be efficiently achieved by using tapered optical fiber [14].

3.2 Mechanical properties

The mechanical property of the structure was studied by finite-element-method (FEM). In the numerical simulations, the beams are clamped at both ends using the fixed boundary conditions. The mechanical motions of the beam are categorized into in-plane and out-of-plane motions. In this study, the fundamental in-plane mode is investigated. Figure 1(b) shows a color plot of the absolute displacement in y -direction of the mode. The deformation of the structure is exaggerated for clear visibility. The part colored by red indicates the absolute displacement of the structure is large. The mechanical frequency of the mode is calculated to be $\Omega_m/2\pi = 95$ MHz with GaAs material properties: density ρ of 5316 kg/m³, Young's modulus E of 85.9 GPa, thermal expansion coefficient α of 5.7×10^{-6} 1/K, specific heat capacity C_p of 550 J/(kg·K), and thermal conductivity κ_{th} of 33 W/(m·K). The resonant frequency is lower than that of a similar Si structure (175 MHz) due to larger ρ and smaller E . This mode has the maximum displacement at $x = 0$, where the optical cavity mode has the electric field maximum. Therefore, the mechanical motion in y -direction efficiently couples to the fundamental optical cavity mode shown in Fig. 1(a).

The investigated doubly clamped beam structure has several dissipative processes. These damping processes are caused by thermoelastic loss, clamping loss, surrounding gas, and so on. The damping of the vibrating structure in air is very large and leads to a very low Q_m of the order of 100. We assume that the optomechanical system is in high vacuum where the gas

damping is negligible as this is the regime where most experimental investigations have been performed. Thermoelastic loss is often the main damping mechanism in the mechanical structure and limits the value of Q_m at room temperature [27, 28]. The value of Q_m is calculated by Zener's theory of thermoelastic damping with the following expression

$$Q_m = \frac{C_p \rho (1 + \Omega_m \tau_{th})^2}{E \alpha T \Omega_m \tau_{th}} \quad (1)$$

where, τ_{th} is the thermal relaxation time $\tau_{th} = C_p \rho w / \pi^2 \kappa_{th}$ of 40 ns for this system. We obtained very high value of $Q_m = 83,800$, which is higher than that for a Si-based same structure by nearly seven times. The details and reason will be discussed in subsection 3.4.

3.3 Optomechanical coupling properties

In this subsection, we discuss the optomechanical coupling between the fundamental optical mode and the in-plane fundamental mechanical mode. The optomechanical coupling factor g_{OM} is the perturbed optical cavity resonance $\Delta\omega_c$ induced by small displacement Δy of the structure and expressed as $d\omega_c/dy$. One can parameterize the optomechanical coupling strength by an effective coupling length L_{OM} , which is described by $L_{OM}^{-1} = \frac{1}{\omega_c} \frac{d\omega_c}{dy}$. The

coupling length can be obtained by perturbation theory for Maxwell's equations with displacement of material boundaries and described by the following expression

$$L_{OM}^{-1} = \frac{1}{2} \frac{\int (q(r) \cdot \vec{n}) \left[\Delta \varepsilon_{12}(r) |E_{\parallel}^{(0)}(r)|^2 - \Delta(\varepsilon_{12}^{-1}(r)) |D_{\perp}^{(0)}(r)|^2 \right] dA}{\int \varepsilon(r) |E(r)|^2 dV}. \quad (2)$$

In this equation, $q(r)$ is a normalized displacement field defined by $q(r) = Q(r)/\Delta y_{\max}$, where Δy_{\max} is the largest displacement amplitude in the structure. \vec{n} is the unit normal vector at the surface of the membrane in the static condition. $\Delta \varepsilon_{12}$ and $\Delta(\varepsilon_{12}^{-1})$ are defined as $\varepsilon_1 - \varepsilon_2$ and $\varepsilon_1^{-1} - \varepsilon_2^{-1}$, respectively. $E_{\parallel}^{(0)}$ and $D_{\perp}^{(0)}$ are the electric field parallel to and the electric displacement normal to the air/semiconductor boundary. The value of g_{OM} is calculated by the electric field distribution and displacement field and estimated to be 991 GHz/nm, which corresponds to $L_{OM} \sim 200$ nm. The obtained coupling strength is about one order of magnitude larger than that obtained in other optomechanical coupling systems without air-slot. The stronger optomechanical coupling stems from the enhancement of the electric field in the narrow air-slot and it clearly indicates great advantage of an air-slot cavity for an optomechanically coupled structures.

3.4 Optical control of a GaAs-based nanomechanical oscillator

We investigated the motion of the nanomechanical oscillator and the time-dependent intensity of the optical cavity mode by numerically solving the coupled equations for the stored energy in the optical cavity $|a|^2$ and the input power $|s|^2$

$$\frac{da}{dt} = i\Delta\omega(y)a - \left(\frac{1}{2\tau_0} + \frac{1}{2\tau_{ex}} \right) a + \sqrt{\frac{1}{\tau_{ex}}} s \quad (3)$$

$$\frac{d^2 y}{dt^2} + \frac{\Omega_m}{2Q_m} \frac{dy}{dt} + \Omega_m^2 y = \frac{F_{OM}}{m_{eff}} = -\frac{g_{OM}}{\omega_c} \frac{|a|^2}{m_{eff}} \quad (4)$$

where $\Delta\omega(y) = \Delta\omega - g_{OM}y$: $\Delta\omega$ is the detuning of the pump laser frequency with respect to the cavity resonance. The cavity field decay rate κ is given by $\frac{1}{2\tau_0} + \frac{1}{2\tau_{ex}}$, where the first term is the intrinsic cavity field decay rate and the second term is the coupling rate to the external system for pumping. The effective mass m_{eff} is computed from the following equation

$$m_{eff} = \int \frac{(r-r_0)^2}{(r-r_0)_{max}^2} \rho dV, \quad (5)$$

where, r is the position of each segment used in the FEM simulation and $(r-r_0)$ is the displacement of the segment from the original position of r_0 at the static condition. The integral is taken over the whole beams and m_{eff} is calculated to be ~ 6 pg. The motion of the optomechanically coupled structure can be simulated by Eqs. (3) and (4) with the obtained parameters. $\Delta\omega$ is crucial parameter to determine how the mechanical system is optically controlled. It is known that blue detuning ($\Delta\omega > 0$) and red detuning ($\Delta\omega < 0$) respectively amplifies and damps the motion of mechanical oscillators. In this work, we mainly discuss the case of the red detuning. The optomechanical coupling modifies the intrinsic mechanical resonator damping rate Γ . In the weak retardation regime ($\kappa \gg \Omega_m$), in our case, the modified damping rate Γ_{om} induced by laser beam with pump power P can be calculated by the following equation [15],

$$\Gamma_{om} = -\frac{\omega_c}{2\Omega_m L_{om}^2 m_{eff}} \left(\frac{2\kappa_{ex}}{\kappa^2 + 4\Delta(y)^2} \right) \left[\frac{\kappa/2}{(\Delta(y) - \Omega_m)^2 + (\kappa/2)^2} - \frac{\kappa/2}{(\Delta(y) + \Omega_m)^2 + (\kappa/2)^2} \right] P. \quad (6)$$

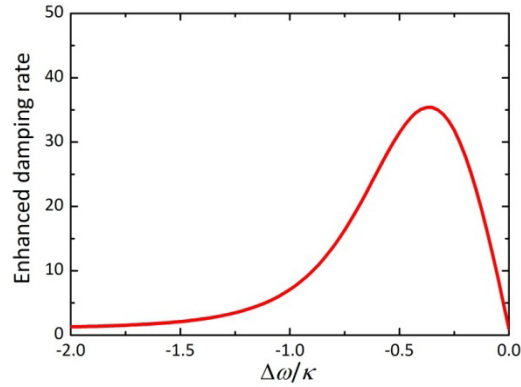


Fig. 2. Enhanced damping rate at various laser frequency detuning with respect to the cavity resonance $\Delta\omega$. The lateral axis is normalized by the optical cavity decay rate κ .

Figure 2 shows the enhanced damping rate defined by $(\Gamma_{om} + \Gamma) / \Gamma$ at various $\Delta\omega$ in the case of $P = 1$ nW and $Q = 5 \times 10^5$ as an example. Although at zero and very large detuning, the pumping laser does not couple with the mechanical mode, when $\Delta\omega \sim \kappa/2$ the motion of the oscillator becomes sensitive to the cavity electric field. In the investigated structure, the result indicates that the optimal $\Delta\omega$ for optomechanical control is $\sim 0.35\kappa$. The value of $\Delta\omega$ is fixed at 0.35κ or -0.35κ in this study.

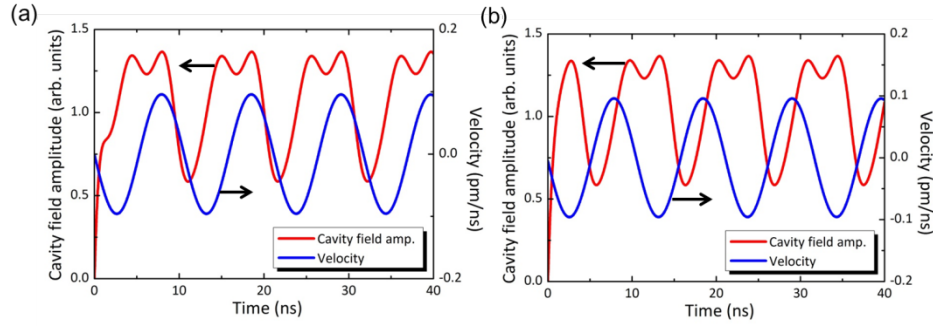


Fig. 3. Time evolution of the velocity of the membrane ($y > 0$) and the cavity field amplitude (a) at the detuning of -0.35κ (red detuning, cooling case) and (b) at the detuning of 0.35κ (blue detuning, heating case).

The cavity field amplitude and the motions of the membrane in the in-plane direction were simulated for the fundamental mode and the results are shown in Figs. 3(a) and 3(b) for the cases of $\Delta\omega = -0.35\kappa$ and 0.35κ . One can see that the cavity field amplitude oscillate at the frequency of the mechanical mode of 95 MHz and there is a π -phase-shift in the cavity field amplitude between the two detuning cases. The right vertical axis is the velocity of the membrane ($y > 0$). When the velocity v is positive, the membrane moves to $+y$ direction and the slit width becomes wider. In Fig. 3(a), for the case of red-detuning, the integrated cavity field amplitude over the time period of $v > 0$ is larger than that taken over $v < 0$. This behavior indicates that the cavity field pulls the membrane to $-y$ direction when the membrane moves to $+y$ direction and results in damping of the mechanical oscillation of the membrane. On the other hand, for the blue-detuning case in Fig. 3(b), the integrated cavity field amplitude over $v > 0$ is smaller than that taken over $v < 0$. Therefore, the amplitude of the mechanical oscillation is amplified by the laser. These results clearly show the laser-induced cooling and amplification of the mechanical motions.

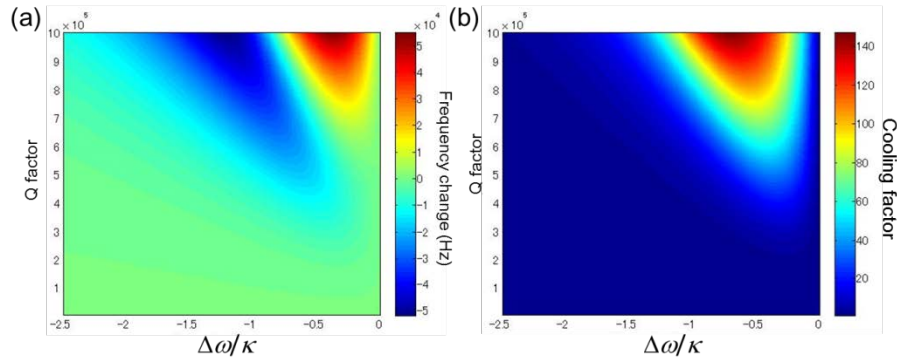


Fig. 4. (a) Mechanical frequency change induced by optical stiffening and (b) cooling factor at various detunings and values of cavity Q at an input power of 1 nW.

The displacement dependent cavity field amplitude leads to optically induced stiffening of the mechanical system, which can be observed as the modification in mechanical eigenfrequency. Figure 4(a) shows calculated mechanical frequencies at various Q s and $\Delta\omega$ s. The mechanical frequency is modified on the order of 10 kHz, which corresponds to $\sim 10^{-4}$ of Ω_m . Figure 4(b) shows cooling factor $F_c = (\Gamma_{om} + \Gamma) / \Gamma$ at various Q s and $\Delta\omega$ s. It is clearly shown that a high- Q optical cavity is essential for optical control of a mechanical oscillator

based on the cavity enhanced scheme and the motion of the oscillator can be optically controlled by precise detuning of $\Delta\omega$.

3.5 Comparison with a Si-based structure

Most of the theoretical and experimental investigations of optomechanics have been done with Si or SiN based structures, because Si-based structures can be processed more precisely compared with III-V semiconductor materials such as GaAs and higher optical cavity Q can be achieved. We also calculated optical and mechanical properties of the investigated structure for Si-based material in the same manner as GaAs-based material. In numerical simulations, the optical property of a GaAs-based and a Si-based air-slot mode-gap PhC nanocavity are about the same due to the similar refractive indices of GaAs (~ 3.4) and Si (~ 3.5) at $1.5\ \mu\text{m}$ range. Here, we note that GaAs has advantageous mechanical properties, which is crucial for optomechanical systems, over Si at room temperature, where thermoelastic loss is the dominant damping mechanism in this system. The value of Q_m was estimated by Zener's theory using Eq. (1) with material parameters summarized in Table 1.

Table 1. Summary of the parameters used to estimate Q_m and values of Q_m for GaAs and Si-based structures.

	E [GPa]	ρ [kg/m ³]	C_p [J/(kg·K)]	α [10 ⁻⁶ /K]	κ [W/(m·K)]	τ_{th} [ns]	Q_m
GaAs	85.9	5316	550	5.7	33	40	83800
Si	130	2330	703	4.15	156	4.8	13300

The values of Q_m for the GaAs-based and the Si-based structures of the investigated design are 83,800 and 13,300, respectively. In the estimation, we found that the higher Q_m of the GaAs-based structure stemmed from a longer thermal relaxation time in a GaAs material. The difference in thermal relaxation times, $\tau_{th} = C_p \rho w / \pi^2 \kappa_{th}$, between GaAs and Si is mainly caused by κ_{th} , which is different by a factor of 8. This thermal feature leads to less thermoelastic loss in the GaAs structure and to better mechanical property.

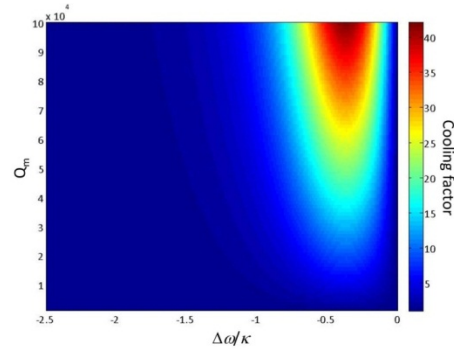


Fig. 5. Color map of the calculated cooling factors at various detunings and values of Q_m at an input power of 1 nW. Cavity Q is fixed at 5×10^5 .

We calculated cooling factors of the investigated structure at various Q_m s in the case of $P = 1\ \text{nW}$ and $Q = 5 \times 10^5$, and the result is shown in Fig. 5. The parameters used in the estimation are those of GaAs material besides Q_m . One can see that F_c strongly depends on Q_m . This result indicates the importance of mechanical property for optomechanical structures. Currently, we fabricate the designed GaAs-based structures and the experimental results will be reported elsewhere.

4. Summary

A GaAs-based optomechanical nanostructure with an air-slot mode-gap PhC nanocavity is theoretically investigated. The GaAs-based structure provides better mechanical property than that of a Si-based structure at room temperature due to lower thermoelastic loss. The importance of less mechanical damping in optical control of nanomechanical oscillators is clearly shown in the simulation. In addition, the GaAs-based structure provides excellent optical property as a Si-based structure due to the similar refractive indices at 1.5 μm wavelength range. Although most of the experimental investigations have adopted Si material to fabricate optomechanical oscillators, obtained simulation results indicate that GaAs also can be a good material for optomechanical structures: the difficulty in the fabrication process is compensated by the superior mechanical properties of GaAs.

Acknowledgments

The author would like to thank K. Hirakawa, W. Shimizu and E. Harbord for helpful discussions. This work was partly supported by Nippon Sheet Glass Foundation for Materials Science and Engineering, the Mitsubishi Foundation, and Project for Developing Innovation Systems of the Ministry of Education, Culture, Sports, Science and Technology (MEXT), Japan.